# Coulomb drag between ballistic one-dimensional electron systems

**P. Debray[1], V. Gurevich[2], R. Klesse[3], R. S. Newrock[4]**

[1] Service de Physique de lÉtat Condensé, CEA Saclay, 91191 Gir-sur-Yvette, France
[2] Solid State Physics Division, A. F. Ioffe Institute, 194021 Saint Petersburg, Russia
[3] Institut für Theoretische Physik, Universität zu Köln, Germany
[4] Department of Physics, University of Cincinatti, Ohio 45221-0011, USA

**Abstract.** The presence of pronounced electronic correlations in a one-dimensional systems strongly enhances Coulomb coupling and is expected to result in distinctive features in the Coulomb drag between them that are absent in the drag between two-dimensional systems. In this article, we review recent Fermi and Luttinger liquid theories of Coulomb drag between ballistic one-dimensional electron systems, alias quantum wires, in the absence of inter-wire tunneling, to focus on these features and give a brief summary of the experimental work reported so far on one-dimensional drag. Both the Fermi liquid (FL) and the Luttinger liquid (LL) theory predict a maximum of the drag resistance $R_D$ when the one-dimensional subbands of the two quantum wires are aligned and the Fermi wave vector $k_F$ is small, and also an exponential decay of $R_D$ with increasing inter-wire separation, both features confirmed by experimental observations. A crucial difference between the two theoretical models emerges in the temperature dependence of the drag effect. Whereas the FL theory predicts a linear temperature dependence, the LL theory promises a rich and varied dependence on temperature depending on the relative magnitudes of the energy and length scales of the systems. At very low temperatures, the drag resistance may diverge due to the formation of locked charge density waves. At higher temperatures, it should show a power-law dependence on temperature, $R_D \propto T^x$, experimentally confirmed in a narrow temperature range, where $x$ is determined by the Luttinger liquid parameters. The spin degree of freedom plays an important role in the LL theory in predicting the features of the drag effect and is crucial for the interpretation of experimental results. Substantial experimental and theoretical work remains to be done for a comprehensive understanding of one-dimensional Coulomb drag.

## 1. Introduction

Moving charge carriers in a conductor exert a Coulomb force on the charge carriers in a nearby conductor and induce a drag current in the latter via momentum transfer. This phenomenon, known as Coulomb drag, was predicted by Pogrebinskii in his pioneering paper [1] in which he argued that in a structure of two semiconductor layers separated by an insulating layer, there would be a drag of carriers in layer 1 ("drag layer"), resulting in a drag current $I_D$, due to the direct Coulomb interaction with the carriers in layer 2 ("drive layer"), where an electric current $I$ flows. If no current is allowed to flow in the drag layer, the charge carriers will accumulate at one end inducing a charge imbalance across the layer. This charge will continue to accumulate until the force of the resulting electric field balances the drag force. In the stationary state there will be an induced or 'drag' voltage $V_D$ in the drag layer. When the carriers in both layers are of the same type (electrons or holes), the drag voltage has a sign opposite to the voltage drop in the drive layer. Figure 1 gives a schematic view of Coulomb drag between two parallel quantum wires. The quantity usually measured in experiments is the drag voltage $V_D$. The drag resistance $R_D$ is defined as $R_D = -V_D\ /I$.

**Figure 1.** Schematic view of Coulomb drag between parallel quantum wires.

Coulomb drag between two-dimensional (2D) electron systems has been extensively studied [2] both experimentally and theoretically. The basic physics involved in the description of the drag in two dimensions is now well understood on the basis of Fermi liquid (FL) theory of interacting fermions. The FL theory is well established in three dimensions, holds marginally for many two-dimensional systems, but generally fails in one-dimension. The theory is based on Landau's conjecture that the low-lying excitations of interacting fermion systems can be connected continuously to those of the non-interacting Fermi gas – there is a smooth mapping between the quasiparticles of the interacting and of the non-interacting system [3].

Coulomb drag between one-dimensional (1D) electron systems has been the focus of considerable interest in recent years because our understanding of the quantum properties in interacting 1D systems is unsatisfactory. Experimental work on the subject remains quite limited [4, 5, 6, 7], a fair number of theoretical papers have been published [8, 9, 10, 11, 12, 13, 14, 15, 16, 17, 18]. The primary reason for this theoretical interest is that Coulomb drag is one of the most effective ways to study electron-electron (e-e) interaction.

It is now theoretically established that in an interacting 1D electron gas of infinite length the e-e-interaction completely modifies the ground state of the system. The elementary excitations can not be treated as non-interacting quasiparticles of a conventional Fermi liquid, but instead acquire a bosonic nature. An adequate theoretical description of these interacting 1D systems can be done in terms of the

so-called Luttinger-liquid (LL) [19] (for a recent review see [20]), complementary to the FL description in higher dimensions. In a real 1D system of finite length at finite temperatures, the extent of influence of the e-e interaction will depend on the system parameters.

Experimental efforts to observe manifestation of Luttinger liquid behavior, however, have been quite limited [21, 22, 23, 24]. Part of the problem is that the (e-e) interaction has little influence on the conductance of a single wire, since the current is proportional to the total electron quasi-momentum, which is conserved in electron-electron collisions. To look for experimental evidence of the LL state it would therefore help to explore a new experimental tool based on new devices and physical phenomena. Coulomb drag between 1D electron systems in a dual-wire configuration and opens up a new opportunity and avenue for experimentally probing the LL state in a 1D electron system.

The purpose of this review paper is to present the current status of the theory of Coulomb drag between 1D electron systems for electron transport in the ballistic regime, and to report on experimental measurements of the 1D drag effect. Ballistic transport takes place when the quantum wire dimensions are smaller than both the elastic and the inelastic scattering lengths. Electron transport is strictly one dimensional when only the lowest 1D subband of the wire is occupied and transport takes place in the fundamental mode. The ballistic regime is well suited for Coulomb drag study, since in this regime other scattering processes, such as impurity and phonon scattering, are either insignificant or totally absent.

Further theoretical and experimental investigation of the 1D Coulomb drag effect can enhance our general understanding of the properties of systems of low dimensionality. This broad class of systems is currently a very active area of research. In addition to its fundamental interest, a comprehensive understanding of Coulomb interaction between quantum wires is expected to play a significant role in the design of nanodevices, such as single-electron transistors (SETs) [25] and quantum cellular automata (QCA) [26], which are comprised of quantum dots and quantum wires in close proximity.

The paper is organized as follows. Section 2 describes the theory of 1D Coulomb drag based on the Fermi liquid approach. Section 3 reviews the Luttinger liquid description of this effect. In Section 4 is presented a summary of the experimental work reported so far and a comprehensive analysis of the experimental results using both the FL and the LL descriptions of 1D Coulomb drag. Finally, Section 5 gives some guidelines for future work on the subject.

## 2. Fermi liquid approach

In this section the 1D Coulomb drag is analyzed within the Fermi-liquid concept. We will follow Refs. [8, 18] and use the physical picture developed by Landauer [28], Imry [29], and Büttiker [30]. We assume that each quantum wire is connected to ideal electronic reservoirs attached to its ends. The relaxation processes in the reservoirs are considered

to be so fast that each of them is in thermal equilibrium.

The e-e interaction within a single quantum wire does not result in a current variation because of the quasimomentum conservation in the e-e collisions. However, if two such wires, 1 and 2 are near one another and are parallel, the Coulomb interaction of electrons belonging to different wires can transfer momenta between the wires, which eventually gives rise to a drag effect.

The drag force due to the ballistic current in wire 2 creates a sort of permanent acceleration on the electrons of wire 1. As wire 1 has a finite length $L$ a steady drag current $J$ is established.

Within the Fermi liquid approach we restrict ourselves to direct electron-electron collisions mediated by the Coulomb interaction. Let us analyze the conservation laws for such collisions of electrons belonging to two different wires, 1 and 2, each of them being parallel to the $x$-axis. We have

$$\epsilon^{(1)}_{nk} + \epsilon^{(2)}_{n'k'} = \epsilon^{(1)}_{l,k+q} + \epsilon^{(2)}_{l',k'-q} \tag{1}$$

Here $\hbar k$ is the $x$-component of the of the electron quasimomentum. In this and the next sections we will put $\hbar = 1$ and $k_{\rm B} = 1$ (where $k_{\rm B}$ is the Boltzmann constant). These quantities will be restored only in some final (or most important) formulas. Now,

$$\epsilon^{(1,2)}_{nk} = \varepsilon^{(1,2)}_{n}(0) + k^2/2m, \tag{2}$$

$m$ being the effective mass while $n$ being the transverse quantization subband (channel) index, with primed quantities corresponding to wire 2 throughout. The solution of Eq. (1) can be written as

$$q = -(k-k')/2 \pm \sqrt{(k-k')^2/4 + m\delta\varepsilon} \tag{3}$$

with $\delta\varepsilon = \varepsilon^{(1)}_{n}(0) + \varepsilon^{(2)}_{n'}(0) - \varepsilon^{(1)}_{l}(0) - \varepsilon^{(2)}_{l'}(0)$.

We assume that the electrons of the quantum wires are degenerate and the temperature is low compared to the electron Fermi energy. For the electron-electron collision to be possible, the absolute values of the four quantities, namely, $\epsilon^{(1)}_{nk}, \epsilon^{(2)}_{n'k'}, \epsilon^{(1)}_{l,k+q}$, and $\epsilon^{(2)}_{l',k'-q}$ should be within the stripes $k_{\rm B}T$ near the corresponding Fermi levels. This means that within the accuracy $mT/k_F$ the following relations should be valid

$$\begin{aligned} k \qquad &= k^{(n)}_F, \quad k' = k^{(n')}_F, \\ |k+q| &= k^{(l)}_F, \quad |k'-q| = k^{(l')}_F. \end{aligned} \tag{4}$$

Here $k^{(n)}_F$ denotes the Fermi quasimomemtum for band $n$. In general it is impossible by variation of a single quantity, i.e. the transferred quasimomentum $q$, to satisfy both relations of Eq. (4) (provided, of course, that the distances between the channel bottoms are much bigger than $T$.)

In other words, one cannot in general satisfy Eq. (1) for a finite $\delta\epsilon$. Therefore for a general case one should have $n = l, \quad n' = l'$. If both wires are identical equations $n = l', \quad n' = l$ are also possible. In both cases $\delta\epsilon = 0$. We will assume the wires to be different. Then

$$\delta(\epsilon^{(1)}_{nk} + \epsilon^{(2)}_{n'k'} - \epsilon^{(1)}_{l,k+q} - \epsilon^{(2)}_{l',k'-q}) = (m/|q|)\delta(k-k'+q). \tag{5}$$

This means that the quasimomentum transferred during a collision is $q = k' - k$, i.e. the electrons swap their quasimomenta as a result of collision.

Assuming that the drag current in wire 1 is much smaller than the ballistic current in wire 2, we calculate the drag current by solving the Boltzmann equation for wire 1 (otherwise we should have solved a system of coupled equations for both wires). We assume the wires to be different though having the same lengths $L$ and consider the interaction processes when electrons in the two quantum wires after scattering remain within the initial subbands $\epsilon^{(1)}_{nk} = \varepsilon^{(1)}_n(0) + k^2/2m$ and $\epsilon^{(2)}_{n'k} = \varepsilon^{(2)}_{n'}(0) + k^2/2m$, $n$ being the subband's number. The Boltzmann equation for the electrons occupying the $n$th subband is

$$v_k \frac{\partial F^{(1)}}{\partial k} = \mathcal{I}^{(12)}\{F^{(1)}, F^{(2)}\} \tag{6}$$

where $F^{(1,2)}$ are the electron distribution functions in wires 1 and 2 respectively, and $I$ is the collision integral. We assume that the only type of collisions that is essential is the interwire $e$-$e$ collisions described by the term

$$\mathcal{I}^{(12)}\{F^{(1)}, F^{(2)}\} = 2 \int \frac{dk'}{2\pi} \int \frac{dq}{2\pi} \sum_{n'} w(1, k+q, n; 2, k'-q, n' \leftarrow 1, k, n; 2, k', n')\mathcal{P} \tag{7}$$

where

$$\mathcal{P} = \left[F^{(1)}_{nk} F^{(2)}_{n'k'} \left(1 - F^{(1)}_{nk+q}\right)\left(1 - F^{(2)}_{n'k'-q}\right) - F^{(1)}_{nk+q} F^{(2)}_{n'k'-q} \left(1 - F^{(1)}_{nk}\right)\left(1 - F^{(2)}_{n'k'}\right)\right]. \tag{8}$$

2 is the spin factor; the scattering probabilities are assumed to be spin-independent. If the e-e collisions can be treated within the perturbation theory then the scattering probability is given by

$$w(1, k+q, n, 2, k'-q, n' \leftarrow 1, k, n; 2, k', n') = 2\pi |\langle 1, k+q, n; 2, k'-q, n'|V|1, k, n; 2, k', n'\rangle|^2 \times \delta(\epsilon^{(1)}_{nk} + \epsilon^{(2)}_{n'k'} - \epsilon^{(1)}_{n,k+q} - \epsilon^{(2)}_{n',k'-q}). \tag{9}$$

The matrix element of electron-electron interaction can be transformed to

$$\langle 1, k+q, n; 2, k'-q, n'|V|1, k, n; 2, k', n'\rangle$$

$$= \frac{1}{L} \int d^2 r_\perp \int d^2 r'_\perp \phi^*_n(\mathbf{r}_\perp)\phi^*_{n'}(\mathbf{r'}_\perp) \times V_q(\mathbf{r}_\perp - \mathbf{r'}_\perp)\phi_n(\mathbf{r}_\perp)\phi_{n'}(\mathbf{r'}_\perp) \tag{10}$$

where $V_q = \int dx V(x, \mathbf{r}_\perp) \exp(-iqx)$, $\mathbf{r}_\perp = (y, z)$. We have

$$\int dx \int dx'\, V(\mathbf{r} - \mathbf{r}') e^{iq(x-x')} = 2e^2 L K_0(|q|\,|\Delta r_\perp|) \tag{11}$$

where $\Delta\mathbf{r}_\perp = \mathbf{r}_\perp - \mathbf{r}'_\perp$ and $K_0$ is a modified Bessel function defined in Ref. [35]. Now,

$$K_0(\xi) = \begin{cases} -\ln(\xi/2), & \xi \ll 1, \\ \sqrt{\pi/2\xi}\, e^{-\xi}, & \xi \gg 1. \end{cases} \tag{12}$$

It means that the $e$-$e$ interaction goes down exponentially provided $|q||\mathbf{r}_\perp - \mathbf{r}'_\perp|/\hbar \gg 1$.

To calculate the current in wire 1 we iterate the Boltzmann equation (6) in the collision term $\mathcal{I}^{(12)}$. The first iteration gives for the nonequilibrium part of the distribution function $\Delta F^{(1)}_{np}$

$$\Delta F^{(1)}_{nk} = -\left(z \pm \frac{L}{2}\right) \frac{1}{v_n} \mathcal{I}^{(12)}\{F^{(1)}, F^{(2)}\} \tag{13}$$

for $k > 0$ ($k < 0$) respectively. One gets for the drag current

$$I_D = -2eL \sum_n \int_0^\infty \frac{dk}{2\pi} \mathcal{I}^{(12)}\{F^{(1)}, F^{(2)}\}. \tag{14}$$

We assume in the spirit of the Landauer-Büttiker-Imry approach the driving wire connected to the reservoirs which we call "left" (+) and "right" (−), each of these being in independent equilibrium. Let the $x$-component of the quasimomentum of an electron in wire 2 before scattering be $k'$, after scattering by an electron of wire 1 be $k' - q$. Let $k' > 0$ while $k' - q < 0$. Then the first distribution function in wire 2 is $F^{(0)}_{n'k} = f(\epsilon^{(2)}_{n'k} - \mu^{(+)})$ where $f$ is the equilibrium Fermi function. The second one is $F^{(0)}_{l',k+q} = f(\epsilon^{(2)}_{l',k+q} - \mu^{(-)})$ where $\mu^{(\pm)} = \mu \pm eV/2$. At $eV = 0$ the wires are in equilibrium. We denote the corresponding equilibrium chemical potential as $\mu$.

Let us denote by $\Delta\{F\}$ the expression one gets after substitution of the equilibrium distribution functions given above into the collision term. For $k' > 0$ ($k' < 0$) and $k' - q < 0$ ($k' - q > 0$) where $k'$ is the electron quasimomentum in wire 2 before the scattering we obtain

$$\Delta\{F^{(1)}, F^{(2)}\} = \pm 2 \sinh\left(\frac{eV}{2T}\right)$$

$$\times [1 - f(\epsilon^{(1)}_{nk} - \mu)][1 - f(\epsilon^{(2)}_{n',k'} - \mu^{(+)})]$$
$$\times f(\epsilon^{(1)}_{n,k+q} - \mu) f(\epsilon^{(2)}_{n',k'-q} - \mu^{(-)}). \tag{15}$$

We begin with a discussion of the Ohmic case $eV/T \ll 1$. Accordingly, we replace $\sinh(eV/2T)$ by its argument and all the chemical potentials in Eq. (15) by the same value $\mu$. The initial and final states of the colliding electrons should be within $T$ of the Fermi levels [8]. This means that only the terms with $\varepsilon^{(1)}_n(0) = \varepsilon^{(2)}_{n'}(0)$ where the equality is satisfied with the indicated accuracy give the principal contribution to the current. (The importance of equal channel velocities was also pointed out in Ref. [9]). The contribution of each such pair of levels to the current is

$$I_D = \frac{e^5 m^3 L k_{\rm B} T e V}{2\pi^2 \kappa^2} \frac{1}{{k_n}^3} g_{nn}(2k_n) \frac{[\varepsilon^{(1)}_n(0) - \varepsilon^{(2)}_{n'}(0)]^2}{4(k_{\rm B}T)^2}$$
$$\times \left[\sinh \frac{\varepsilon^{(1)}_n(0) - \varepsilon^{(2)}_{n'}(0)}{2k_{\rm B}T}\right]^{-2} \tag{16}$$

where

$$g_{nn'}(q) = \left| \int d^2 r_\perp \int d^2 r'_\perp |\phi_n(r_\perp)|^2 |\phi_n(r'_\perp)|^2 K_0(q|\Delta \mathbf{r}_\perp|) \right|^2 , \tag{17}$$

$\kappa$ is the dielectric susceptibility of the lattice, $k_n = \sqrt{2m[\mu - \varepsilon_n(0)]}$. This equation has been also obtained using linear response theory. In the case considered, wire 2 is a part of a usual structure for measuring ballistic conductance, i.e. it joins two classical reservoirs, each of them being in independent equilibrium. The driving current is [29]

$$I = \mathcal{N} \frac{e^2}{\pi} V, \tag{18}$$

$\mathcal{N}$ being the number of active channels (i.e. the subbands whose bottoms are below the Fermi level). So far a simplifying assumption has been used: the chemical potential $\mu$ in wire 1 and the average chemical potential in wire 2 are equal. In the general case they can have different values $\mu^{(1)}$ and $\mu^{(2)}$, respectively. Then one still gets Eq. (16) with the replacement

$$\varepsilon_n^{(1,2)}(0) \to \tilde{\varepsilon}_n^{(1,2)}(0) \equiv \varepsilon_n^{(1,2)}(0) - \mu^{(1,2)}.$$

One can measure either the current or the voltage that builds up in wire 1. The ratio of the drag current to the ballistic driving current for $\tilde{\epsilon}_n^{(1)}(0) = \tilde{\epsilon}_{n'}^{(2)}(0)$ is given by

$$\frac{I}{I_D} = \frac{4e^4 m^3 L k_{\mathrm{B}} T}{\pi \hbar^3 \kappa^2 \mathcal{N}} \sum_{nn'} \mathcal{D}_{nn'} \tag{19}$$

where

$$\mathcal{D}_{nn'} = \frac{1}{\left(k_n^{(1)} + k_n^{(2)}\right)^3} g_{nn'} \left(k_n^{(1)} + k_n^{(2)}\right). \tag{20}$$

Here $k_n^{(1,2)} = \sqrt{2m[\mu^{(1,2)} - \varepsilon_n^{(1,2)}(0)]}$. In this approximation, $k_n^{(1,2)} = k_{n'}^{(1,2)}$. In an experiment one usually measures the drag resistance $R_D = -V_D/I = I_D G_D / I$, where $G_D$ is the ballistic resistance of the drag wire and depends on the number of occupied subbands.

The 1D subband structure of the wires can be modified by changing the effective wire widths by applying appropriate gate voltages (Fig. 5). The variation of gate voltage may affect the positions of the levels of transverse quantization in the two wires in a different way. In the course of such a variation a coincidence of a pair of such levels in the two wires may be reached. The estimate (20) is not very sensitive to the form of confining potential and electron densities. In Fig. 3 the ratio $I/I_D$ is plotted (for $\mu^{(1)} = \mu^{(2)}$) as a function of the ratio of effective wire widths. This plot exhibits striking oscillations with large peak-to-valley ratios. The peaks occur when channel velocities in two interacting wires are equal which happens whenever any two current-carrying channels line up. This sort of coupling is particularly strong when such channel velocities are quite small.

The condition $\tilde{\epsilon}_n^{(1)}(0) = \tilde{\epsilon}_{n'}^{(2)}(0)$ gives the main maxima of the drag current, especially for the lowest levels of transverse quantization. Some subsidiary maxima can also be observed, particularly in external magnetic field — see Ref. [14].

So far we have considered the peaks of the drag current under conditions where the Fermi level is well above the coinciding bands in wires 1 and 2. Now we would like to say a few words about a special case that may be particularly important regarding the experiment described below. This is the case where the bottoms of two subbands not only coincide but also just touch the Fermi level. Then the conduction electrons obey the so-called *intermediate statistics*. It means that their equilibrium distribution functions are

$$f = \frac{1}{\exp(k^2/2mT) + 1} \tag{21}$$

The drag current is proportional to the e-e scattering probability averaged over this distribution function. The scattering probability itself is determined by the quantum mechanics, i.e. it depends on the form of electron wave function in the quantum wire, in other words, on the exact form of the confining potential. Investigation of the temperature dependence of the drag in this special case is one of the problems of the theory to be solved in future.

Now we turn to the case of non-Ohmic transport in the drive wire, i.e. to the case where $eV \gg k_{\mathrm{B}}T$ [18]. The situation for $\mu^{(1)} = \mu^{(2)}$ is illustrated in Fig. 2. The upper and the lower dashed lines correspond to the positions of the chemical potentials $\mu^{(-)}$ and $\mu^{(+)}$, respectively, while the middle dashed line corresponds to the average value $\mu$. Parabolas (1) and (2) represent the dispersion law of electrons in wires 1 and 2 respectively. The full circles correspond to the initial states of colliding electrons.

*Before the collision* states 1a and 2a are occupied. The circle representing state 1a is below the dashed line, i.e. below the Fermi level $\mu$. The circle 2a represents a state with $p > 0$, which is also occupied as the corresponding energy is below $\mu^{(+)}$.

*After the collision* state 1b is occupied. It is represented by a circle above the dashed line, which means that it has been free before the collision. In wire 2 state 2b with $p < 0$ is also occupied. It is above $\mu^{(+)}$, i.e. it had been free before the transition.

The width of the stripe between the two straight lines is $eV$. If the bottoms of the active subbands are well below the Fermi level the drag current should be proportional to the number of the occupied initial states as well as to the number of free final states.

To calculate the drag current, one can recast the product of distribution functions in the collision term Eqs. (7) and (8) into the form

$$\mathcal{P} = 2\sinh(eV/2T)\mathcal{Q} \tag{22}$$

where

$$\begin{aligned}\mathcal{Q} = \exp\frac{\varepsilon_{nk}^{(1)} - \mu}{T} \exp\frac{\varepsilon_{n'k'}^{(2)} - \mu}{T} f(\varepsilon_{nk}^{(1)} - \mu) f\left(\varepsilon_{n'k'}^{(2)} - \mu^{(+)}\right) \\ \times f(\varepsilon_{nk'}^{(1)} - \mu) f\left(\varepsilon_{n'k}^{(2)} - \mu^{(-)}\right).\end{aligned} \tag{23}$$

For the drag current one gets

$$I = -\sinh\left(\frac{eV}{2T}\right)\frac{8e^5mL}{\pi^2\kappa^2}\times\sum_{nn'}\int_0^\infty dk\int_0^\infty dk'\frac{g_{nn'}(k+k')}{k+k'}\mathcal{Q}. \tag{24}$$

As above, one can conclude that the terms which give the main contribution to the drag current are those where $|\tilde{\varepsilon}_n^{(1)}(0)-\tilde{\varepsilon}_{n'}^{(2)}(0)|$ is smaller than or of the order of $k_{\rm B}T$ or $eV$. We will assume that there is only one such difference (otherwise we would have got a sum of several terms of the same structure).

As $\mathcal{Q}$ is a sharp function of $k$ and $k'$, one can take out of the integral all the slowly varying functions and get (the result is given for the general case where $\mu^{(1)}\neq\mu^{(2)}$)

$$I = I_0\cdot\frac{1}{2}\sinh\left(\frac{eV}{2k_{\rm B}T}\right)\frac{\dfrac{eV}{4k_{\rm B}T}-\dfrac{\tilde{\varepsilon}_{nn'}}{2k_{\rm B}T}}{\sinh\left(\dfrac{eV}{4k_{\rm B}T}-\dfrac{\tilde{\varepsilon}_{nn'}}{2k_{\rm B}T}\right)}\times\frac{\dfrac{eV}{4k_{\rm B}T}+\dfrac{\tilde{\varepsilon}_{nn'}}{2k_{\rm B}T}}{\sinh\left(\dfrac{eV}{4k_{\rm B}T}+\dfrac{\tilde{\varepsilon}_{nn'}}{2k_{\rm B}T}\right)} \tag{25}$$

where

$$I_0 = -\frac{64e^5m^3L(k_{\rm B}T)^2}{\kappa^2\pi^2\hbar^4}\mathcal{D}_{nn'}. \tag{26}$$

Here $\tilde{\varepsilon}_{nn'}=\tilde{\varepsilon}_n^{(1)}(0)-\tilde{\varepsilon}_{n'}^{(2)}(0)$.

For $eV\ll k_{\rm B}T$ Eq. (25) turns into Eq. (16). Let us consider the opposite case $eV\gg k_{\rm B}T$. One gets for the drag current

$$I = \mathcal{B}\left[\left(\frac{eV}{2}\right)^2-(\tilde{\varepsilon}_{nn'})^2\right],\quad \mathcal{B}=-\frac{16e^5m^3L}{\kappa^2\pi^2\hbar^4}\cdot\mathcal{D}_{nn'}. \tag{27}$$

This result is nonvanishing only if $|\tilde{\varepsilon}_{nn\prime}|<eV/2$.

In this Section we have discussed a Fermi liquid theory of the Coulomb drag current in a quantum wire brought about by a current in a nearby parallel quantum wire. A ballistic transport in both quantum wires is assumed. The drag current $I_D$ as a function of the wire widths comprises one or several spikes; the position of each spike is determined by a coincidence of a pair of levels of transverse quantization, $\varepsilon_n(0)$ and $\varepsilon_{n'}(0)$ in both wires.

**Figure 2.** Schematic representation (for $\mu^{(1)}=\mu^{(2)}$) of simultaneous transitions due to the interaction between electrons of the two wires for $eV\gg k_{\rm B}T$. Circles $\circ$ and $\bullet$ represent the initially unoccupied and occupied states respectively

**Figure 3.** $I/I_D$ is plotted (for $\mu^{(1)}=\mu^{(2)}=\mu$) as a function of $W_1/W_2$ where the width of wire 1 is controlled through gate voltage ($\mu=14\,$meV, $T=1$ Kelvin, $W_2=42\,$nm, $L=1\,\mu$m, $\kappa=13$ and the spacing between wires is $50\,$nm).

## 3. Luttinger Liquid Theory of Coulomb Drag

In 1D systems e-e interaction gives rise to electronic correlations that are believed to destroy the Fermi liquid. Instead, a different state is generated that is usually described as a Luttinger liquid [37, 19] (for reviews see e.g. [20, 38, 39, 40]). It is therefore not surprising that in 1D systems e-e interaction affects the drag in a different way than in two- or three dimensional systems. Indeed, in 1D systems interaction strongly enhances the effect, getting stronger the lower the temperature. As a result, the positive temperature characteristic of the drag resistance from Fermi liquid theory can become a negative one. For sufficiently long wires the drag resistance becomes exponentially large at low temperatures.

This chapter reviews in the main part the works [15, 16, 17], and is organized as follows: Sec. 3.1 introduces bosonic variables as the appropriate language for the discussion to follow. In Sec. 3.2 the renormalization group method is employed in order to show that and in which way the drag becomes enhanced by electron correlations. This consideration will also clarify some relevant energy and length scales of the problem. Sec. 3.3 elaborates on the influence of the electron spin on the drag, while Sec. 3.4 deals with non-linearities and asymmetric double-wires. The last section of this chapter, Sec. 3.5, briefly discusses the drag in a system with a finite region of interaction.

### *3.1. Bosonic variables*

For treating interactions it is convenient to describe excitations of the many-electron system in terms of collective coordinates: for example by the displacement $\varphi(x)$ of electrons. They are normalized in such a way that density and current fluctuations are given by $\partial_x\varphi(x) = -\sqrt{\pi}(n(x) - n_0)$ and $\partial_t\varphi(x) = \sqrt{\pi}I(x)/e$. Rewriting the Hamilton of an interacting 1D electron gas in $\varphi(x)$ and its canonical conjugated field $\Pi(x)$ yields the Hamiltonian of an elastic string

$$H = \frac{v}{2}\int dx K\Pi^2 + \frac{1}{K}(\partial_x\varphi)^2 \,. \tag{28}$$

The stiffness or interaction parameter $K$ and the velocity $v$ are determined by the parameters of the electronic system. For non-interacting electrons $K = 1$, $v = v_F$, while for a system with repulsive interaction $0 < K < 1$ and $v \approx v_F/K$. The solutions $\varphi(x,t)$ of the Hamiltonian (28) are 1D waves with wave velocity $v$. In the limit of strong interactions $K \ll 1$, these solutions correspond to the plasma oscillations of the electron density. Contrary to the underlying fermionic operators, the fields $\varphi$ and $\Pi$ obey bosonic commutation relations. The substitution of the former by the latter is therefore known under the name of "bosonization" [19, 20, 38, 39, 40].

Excitations of a double wire can be similarly described by the respective displacement fields $\varphi_1(x)$ and $\varphi_2(x)$ of each wire. Assuming a symmetrical system, the two eigenmodes of the density oscillations (at a given wavenumber $q$) are the symmetric mode $(+)$, where the density in both wires oscillate in phase, and the anti-symmetric mode $(-)$, where the phases of the density oscillations differ by $\pi$. A Transformation

to the corresponding displacement fields $\phi_\pm = (\varphi_1 \pm \varphi_2)/\sqrt{2}$ decouples the Hamiltonian into a symmetric and anti-symmetric part,

$$\begin{aligned} H &= H_1 + H_2, \\ H_\pm &= \frac{v_\pm}{2} \int dx\, K_\pm \Pi^2 + \frac{1}{K_\pm} (\partial_x \phi_\pm)^2 \,. \end{aligned}$$

Each part has its own set of parameters. In good approximation

$$K_\pm = \left( 1 + \frac{V_0 \pm \bar{V}_0}{\pi v_F} - \frac{V_{2k_F}}{\pi v_F} \right)^{-1/2} , \tag{29}$$

and $v_\pm = v_F/K_\pm$, where $V_0, \bar{V}_0$ are the Fourier transforms of intra-wire and inter-wire interaction $V(x)$ and $\bar{V}(x)$ for small momentum $q \to 0$. $V_{2k_F}$ is the intrawire backscattering strength ($\delta q = 2k_F$) [17]. For the range of applicability of expression (29) see Refs. [41, 42], where more precise estimates of the Luttinger-liquid parameters are given.

So far interwire backscattering of electrons, where a large momentum of order $\delta q = 2k_F$ is exchanged, has not been taken into account. As pointed out in the previous chapter, this coupling however is essential for the drag and must be incorporated in the description. Fortunately, this can be also done in terms of the displacement field, leading to

$$H_b = \lambda \frac{E_0^2}{\pi v_F} \int dx \cos(\sqrt{8\pi}\phi_-) \,. \tag{30}$$

The energy $E_0$ is of order of the Fermi energy, and the dimensionless coupling $\lambda$ is given by

$$\lambda = \frac{\bar{V}_{2k_F}}{2\pi v_-} \,, \tag{31}$$

Note that the symmetric and anti–symmetric modes remain still decoupled. There is no corresponding term in the intra-wire interaction. The reason is that the backscattering within a wire appears as the exchange part of the forward scattering ($\delta q \to 0$), and therefore can be absorbed in the parameters $K_\pm$ and $v_\pm$ (cf. Eq. (29)).

The origin of the backscattering Hamiltonian $H_b$ becomes clear in the limit of strong repulsive intra–wire interaction. In this case the electrons of each wire form well-correlated states with charge densities periodic in $2\pi/k_F$. Accordingly, their local interaction energy is $2\pi$–periodic in the relative displacement $(s_1 - s_2)k_F = \sqrt{8\pi}\phi_-$ The integral over $\cos\sqrt{8\pi}\phi_-(x)$ with an appropriate prefactor therefore gives to first order the corresponding part of the total energy.

### *3.2. Drag*

The backscattering Hamiltonian (30) is of sine-Gordon type, and allows for an intuitive understanding of the drag in the case of large couplings $\lambda$. Suppose that the total energy is dominated by $H_b$, the system minimizes its energy by fixing the field $\phi_-$ to a value $\sqrt{8\pi}\phi_0 = \pi + 2\pi m$, $m$ an integer number. Accordingly, the relative displacement of

electrons in wire 1 and 2 is constant in time and space. This means that two interlocked charge density waves have been formed, such that a current in one wire is necessarily accompanied by an equally large current in the second wire. In this ideal situation the drag is absolute [15].

What happens to the drag if the situation is not that ideal is the issue of this section. Considerable insight with a minimum of calculation effort will be gained by making use of the concept of renormalization.

Neglecting for a while all interactions except for the inter-wire backscattering, the double wire system can be viewed as a pair of uncorrelated 1D Fermi liquids. As explained in the previous section, the inter-wire backscattering coupling then causes a drag resistivity $\rho_D = R_D/L$, where $L$ is the length of the drag wire, linear in temperature and proportional to $\lambda^2$,

$$\rho_D \approx \rho_0 \lambda^2 T/E_0 \tag{32}$$

(cf. Eq. 16 in the limit of $T \gg \Delta\varepsilon_n(0)$). To first order the drag only depends on the direct backward scattering part of the interaction. However, higher order contributions to $\rho_D$ include inter- and also intra-wire forward scattering. In 1D these higher order contributions are crucial and must be taken into account. The renormalization group theory does the job quite elegantly by successively integrating out high energy degrees of freedom down to an energy scale $E < E_0$. As a result, the original ("bare") couplings $K_-$, $\lambda$ become renormalized to $E$–dependent couplings $K_-(E)$ and $\lambda(E)$. The energy scale at which the renormalization procedure has to be stopped can be given either by the temperature, the system size, or even by the coupling $\lambda(E)$ itself, depending on the circumstances. The net effect of higher order processes on the drag between a pair of weakly coupled wire can be summarized by replacing – for example in Eq. (32) – the bare coupling $\lambda$ by a renormalized energy dependent ("running") coupling constant $\lambda(E)$. Further, good approximations for relevant energy scales can be easily extracted from the renormalization procedure. This should be enough motivation for a short excursion to the renormalization flow of the sine-Gordon model.

*3.2.1. Renormalization flow* The flow is well-known from a closely related problem, that of an interacting spin-1/2 electron liquid [44]. For small couplings $\lambda \ll 1$ it is described by the differential equations

$$\frac{d\lambda}{dt} = (2 - 2K)\lambda, \quad \frac{dK}{dt} = -2\lambda^2 K^2, \tag{33}$$

where $t$ denotes the negative logarithm of the rescaled energy, $t = \ln E_0/E$. (The subscript "$-$" is suppressed henceforth.) Fig. 4 shows schematically the flow in a $K - \lambda$–diagram. Each point represents a system characterized by the parameters $K$ and $\lambda$. Under renormalization the system develops according to the stream lines in the parameter space. The arrows indicate the direction of decreasing energy scale.

The main feature of the flow is the so–called Kosterlitz-Thouless transition: systems with parameter below the line $K = 1 + \lambda$ renormalize towards weaker backward

**Figure 4.** The RG-flow of a double wire system of spin-less electrons. Point A corresponds to the bare couplings of a double wire with a rather large inter-wire distance $d \gg \lambda_F$, point B to wires with narrow spacing $d \ll \lambda_F$. Point C corresponds to a single spin-1/2-liquid.

scattering $\lambda$, systems above or left of this line renormalize towards larger $\lambda$. Systems right on the transition line flow to the point at $K = 1$ and $\lambda = 0$, which represents a non-interacting Fermi liquid.

Whether a system develops to weaker or stronger couplings $\lambda$ obviously depends on the location of the bare coupling (subscript "0"), the initial points of the renormalization trajectories. For systems with symmetrical interaction, $V(x) = \bar{V}(x)$, as it is the case for a spin-1/2 electron liquid, one finds for small $V_{2k_F}$ that $K_0 = 1+\lambda_0$, i.e. the initial point lies exactly on the transition line. These systems (marginally) renormalize towards the non-interacting Fermi-point. This is indeed the expected behaviour for the spin-mode of an electron liquid. (The spin-mode corresponds to the anti-symmetric mode $(-)$.) If one could measure the relative drag of spin-up and spin-down electrons, one would find that due to the additional temperature dependence in $\lambda(T)$, the drag resistivity decays with temperature even faster than the naively expected linear behaviour.

Interestingly, the situation is completely different for a real double-wire system. Due to the spatial separation of the two wires, the intra-wire interaction $V(x)$ always exceeds the inter-wire interaction $\bar{V}(x)$. Inspection of Eq.s (29) and (31) reveals that as a consequence the initial point is always above or left of the transition line, where $\lambda$ renormalizes to higher values. Therefore here the backscattering coupling $\lambda$, although usually much smaller than in the previous case, increases with decreasing energy scale or temperature. Hence, for low temperatures (and long wires, see below) the drag resistivity will be always larger than predicted by Fermi theory. This will be made more quantitatively in the next paragraph.

*3.2.2. Temperature dependence of the drag* Before rushing into a discussion of the various kinds of regimes with different types of temperature dependencies, it is advisable to clarify the relevant energy and length scales. There is $E_0 \sim E_F$, the largest energy scale, the temperature $T_L$, at which the thermal wavelength becomes of the order of the system size, and the actual temperature $T$. The corresponding length scales are the Fermi wavelength $\lambda_F \sim E_0/v$, the system size $L$, and the thermal wavelength $L_T = v/T$. Less obviously, a fourth energy and length scale are given by the sine-Gordon Hamiltonian $H_- + H_b$: the energy (mass) $M$ of a soliton and its width $L_s$. The soliton mass $M$ coincides with the energy scale at which the renormalization procedure breaks down, the soliton width $L_s$ is the corresponding length scale. The relative order of these scales classify several different regimes.

For high temperatures $T > T_L, M$, the renormalization of $\lambda$ is terminated by $T$. Thus, $\lambda = \lambda(T)$. In this case the temperature dependence of $\lambda(T)$ can be approximately

determined by integrating the flow equations (33), leading to

$$\lambda(T) = \lambda_0 \left(\frac{T}{E_0}\right)^{2K-2} . \tag{34}$$

This result inserted in Eq. (32) gives the temperature dependence,

$$\rho_D \approx \rho_0 \lambda_0^2 \left(\frac{T}{E_0}\right)^{4K-3} , \tag{35}$$

valid for $T_L, M \ll T \ll E_0$. The e-e interaction changes via the renormalization of the backscattering coupling, the linear temperature dependence known from the 1D Fermi-liquid to a temperature scaling with an interaction dependent power $\chi = 4K - 3$. For sufficiently strong interaction $K$ can assume values below $3/4$. Then the power $\chi$ becomes negative and the drag increases with decreasing temperature. For vanishing interaction, $K = 1$, Eq. (35) goes over to the linear behaviour of the Fermi-liquid.

Lowering the temperature below $M$ or $T_L$, two scenarios are possible: if the wire is sufficiently long, $L \gg W$, at a temperature $T \sim M$ the system eventually enters the strongly coupled regime, where $\lambda(T) \sim 1$. For short wires, $L \lesssim L_s$, this regime can not be reached. Here the renormalization halts at a temperature $T \sim T_L$, where the thermal wavelength is of order the system size. In this case even at low temperatures the systems are weakly coupled, $\lambda(T_L) \ll 1$.

In the strongly coupled regime the energy is dominated by the backscattering term $H_b$, giving rise to an almost absolute drag. Deviations from this ideal drag correspond to processes where the relative displacement $\sqrt{8\pi}\phi_-$ slips from one global minimum position, say at $\pi$, to a neighbouring one at $-\pi$ or $3\pi$. At temperatures $T < M$ these processes are enabled by thermally activated solitons moving along the wire. As a result the drag resistivity shows for $T < M$ an activated behaviour,

$$\rho_D(T) \sim \tilde{\rho}_0 e^{M/T} .$$

This behaviour changes again when the temperature falls below $T_L$ (for the strong coupling regime considered, $T_L < M$). It has been shown [16] that then the drag decreases linearly with temperature, due to the set-in of coherent soliton-tunneling. At even lower temperatures $T < \sqrt{T_L M} \exp -M/T_L$ the drag decreases with $T^2$ [16].

In the weakly coupled regime, the drag resistance decays $\propto T^2$ as the temperature drops below $T_L$. This can be understood as follows: having renormalized down to an energy $T_L$, the original Fermi wavelength length $\lambda_F \sim v/E_0$ has become enlarged to a rescaled wavelength $\lambda_F(T_L) \sim v/T_L = L$. Hence, the wires of length $L$ have effectively shrunk down to pointlike constrictions connecting electronic reservoirs on either side. The drag in this situation is equivalent to the drag in a pair of 1D Fermi-liquids ($K = 1$) that interact over a short length $\lesssim L_T$ only. As it will become clear in the Sec. 3.5, the drag is then proportional to $T^2$ (cf. Sec. 3.5, $K = 1$).

The temperature scale $T_*$ at which the system enters the strongly coupled regime is given by the soliton mass $T_* = M$. Estimating it by $\lambda(T_*) \sim 1$ with the approximate expression (34) yields

$$T_* \sim E_0 \, \lambda^{\frac{1}{2-2K}} . \tag{36}$$

The minimum wire length required is then $L_* = v/T_* = \lambda_F \lambda^{-\frac{1}{2-2K}}$.

### *3.3. Electron Spin*

For comparison to experiments the treatment of the electron spin is mandatory. To this end one can introduce bosonic fields $\varphi_{c/s}$ that are related to the charge/spin density $n_c = n_\uparrow \pm n_\downarrow$ in the same way as above $\varphi$ is related to the density $n$ of spinless particles. For a double wire, this results in a total of four modes: symmetric and anti-symmetric charge modes ($c+$ and $c-$) as before, and, additionally, symmetric and anti-symmetric spin modes ($s+$ and $s-$). Each mode is again described by a quadratic Hamiltonian of the type (28) with corresponding interaction parameters $K_{c\pm}, K_{s\pm}$, etc. . The neutral spin-modes are not affected by the interaction, wherefore $K_{s\pm} = 1$ and $v_{s\pm} = v_F$. Nevertheless, despite their neutrality, the spin-modes weakly couple to the anti-symmetric charge mode $c-$ via backscattering processes. Hence, the drag is influenced by the spin degree of freedom [17].

A quantitative analysis of the weakly coupled regime can again be done by making use of renormalization along the lines described above. The main results are summarized below: In the presence of spin the interwire backscattering coupling scales towards stronger couplings. However, fluctuations in the neutral spin-modes moderate the enhancement due to the interactions. This is reflected by an effective interaction parameter

$$K_{eff} = \frac{K_{c-} + K_{s\pm}}{2} = \frac{K_{c-} + 1}{2}$$

which is closer to the non-interacting value 1 than the original $K_{c-}$. The parameter $K_{c-}$ is given by

$$K_{c-} \approx \left(1 + 2\frac{V_0 - \bar{V}_0}{\pi v_F} - \frac{V_{2k_F}}{\pi v_F}\right)^{-1/2} . \tag{37}$$

As a result, in the weakly coupled regime the drag resistance scales with temperature as

$$\rho_D \approx \rho_0 \lambda_0^2 \left(\frac{T}{E_0}\right)^{2K_{c-}-1}$$

(cf. Eq. (35)). The cross-over temperature $T_*$ turns out to be approximately

$$T_* \sim E_0 \, \lambda^{\frac{1}{1-K_{c-}}} .$$

Comparison with Eq. (36) reveals again the moderating effect of the spin. If two systems have similar interaction constants $K_- \approx K_{c-}$, but one is spin-polarized while the other is not, their respective cross-over temperatures and lengths are related by

$$\left(\frac{T_*}{E_0}\right)^2_{pol.} \approx \left(\frac{T_*}{E_0}\right)_{un-pol.}, \quad \left(\frac{\lambda_F}{L_*}\right)^2_{pol.} \approx \left(\frac{\lambda_F}{L_*}\right)_{un-pol.} .$$

Since $T_*/E_0 \sim \lambda_F/L_*$ is usually a small number, the cross-over temperature of the spin-unpolarized system is by orders of magnitudes smaller than the one of a comparable spin-polarized system.

### *3.4. Non-linear drag and mismatching Fermi-momenta*

So far our considerations were confined to the linear regime ($I \to 0$) of a symmetrical double wire system. This section extends the discussion to both the non-linear regime, and to systems with a misfit in the Fermi momenta, $\delta k = k_{F1} - k_{F2} \neq 0$.

It is again useful to look first at the associated energies. A finite current $I$ in the active wire defines an energy $\Omega = I/e$, and the energy associated to the misfit is of course $\Delta = v\delta k$. Non-linearities of the drag voltage $V_D$ in the current $I$, or an effect of the misfit $\delta k$ will be significant only if the corresponding energies $|\Omega|$ or $|\Delta|$ exceed $T$, $T_L$ and $M$.

In the weakly coupled regime both cases can be analyzed by perturbative methods. Finite currents and a non-vanishing $\delta k$ can be treated by a transformation $\phi(x,t) \to \phi(x,t) + \Delta x/v + \Omega t$. The term linear in $x$ describes the density difference ($\partial_x \phi \propto (n_1 - n_2)$), the term linear in $t$ corresponds to a Galilei boost of the active wire. Accordingly, $H_b$ becomes

$$H_b = \lambda \frac{E_0^2}{\pi v_F} \int dx \, \cos\sqrt{8\pi}(\phi + \Delta x/v + \Omega t) \, .$$

It is possible to derive a closed expression for the drag voltage $V_D$ as a response to this perturbation [43]. It is valid for arbitrary ratios $\Omega/\Delta$, and can be written as

$$\begin{aligned} \frac{eV_D}{L} = C\frac{E_0^2\lambda_0^2}{v}\left(\frac{T}{E_0}\right)^{4K} &\{A(\Omega-\Delta)B(\Omega+\Delta) \\ &+ A(\Omega+\Delta)B(\Omega-\Delta)\} \, . \end{aligned} \tag{38}$$

$C$ is a numerical constant of order unity, $A$ and $B$ are temperature dependent functions, given by

$$A(E) = \int ds \, i\sin(\frac{E}{E_0}s)\left(\pi(\frac{1}{s}+i)\sinh\frac{Ts}{\pi E_0}\right)^{-2K} \, ,$$

and a similar expression with cos instead of $i\sin$ for $B$. This expression holds also for vanishing $\Delta, \Omega$, where it leads to the result (35). For current and $\delta k$ large compared to temperature, $\Omega, \Delta \gg T$, Eq. (38) reduces to [15]

$$\begin{aligned} \frac{eV_D}{L} &= const.\ \lambda_0^2 \, (\Omega^2 - \Delta^2)^{2K-1}, \qquad \text{for } |\Delta| < |\Omega| \\ &= 0 \qquad\qquad\qquad\qquad \text{otherwise} \ . \end{aligned}$$

For non-vanishing $\Delta$ the drag vanishes as long as the current is below a threshold value. For larger currents the voltage shows a powerlaw dependence on the current. A thorough discussion of the non-linear $I-V$ characteristic can be found in [15].

Actually, at finite temperatures the drag does not vanish completely for $|\Delta| > |\Omega|$, rather it shows an activated behaviour as like in the case of 1D Fermi liquids. This can be made more explicit [43]. Evaluating expression (38) in the limit $\Omega \to 0$ at finite $\Delta$ results in a drag resistivity

$$\rho_{\Delta,T} = \rho_0 \lambda^2 \left(\frac{T}{E_0}\right)^{4K-3} F_{2K}(\Delta/T) \, , \tag{39}$$

where $F_{2K}$ is an interaction dependent function defined by

$$F_{2K}(\varepsilon) = N_{2K}(\varepsilon)\frac{dN_{2K}}{d\varepsilon}(-\varepsilon) + N_{2K}(-\varepsilon)\frac{dN_{2K}}{d\varepsilon}(\varepsilon)\,,$$
$$N_{2K}(\varepsilon) = \lim_{\delta\to 0}\int ds\, e^{is\varepsilon/\pi}\left((\frac{\delta}{s}+i)\sinh s\right)^{-2K}\,.$$

$F_{2K}$ is a continuous function. It decays exponentially at large positive arguments, $F_{2K}(\varepsilon) \sim \exp -\varepsilon$, and behaves algebraically for large negative arguments, $F_{2K}(\varepsilon) \sim |\varepsilon|^{K-1}$. The result obtained for non-interacting 1D Fermi-liquids is recovered by putting $K = 1$. In this case

$$N_2(\varepsilon) = \frac{1}{\pi}\frac{\varepsilon}{e^{\varepsilon}-1}\,,$$

such that the expression (39) corresponds to Eq. (16). While $N_2(\varepsilon)$ bears some resemblance to the Bose distribution, for the special interaction parameter $K = 1/2$ one obtains exactly the Fermi function

$$N_1(\varepsilon) = \frac{1}{e^{\varepsilon}+1}\,.$$

For general parameter $K$ an analytical expression for $N_{2K}$ is lacking. It is an open question whether the functions $N_{2K}$ are related to the exclusion statistics of fractional excitations in the Luttinger liquids.

### *3.5. Finite interaction region*

Double wires that interact only over a region of finite length $l < L$ have been also investigated [12, 13]. For temperatures $T < v/l$ this problem can be mapped to the classical problem of a Luttinger liquid with a single impurity. Qualitatively, these systems behave similar to those considered in the previous sections. In the weakly coupled regime the drag scales with temperature with an interaction dependent exponent, $4K - 2$. A strongly coupled regime with almost absolute drag at zero temperature exists as well. However, it is reached only for sufficiently strong interaction $K < 1/2$. For $K > 1/2$ the interwire backscattering coupling renormalizes to weaker couplings, such that the drag vanishes for $T \to 0$.

## 4. Experimental search for 1D Coulomb drag

Although a fair amount of theoretical work has been available on Coulomb drag between 1D electron systems, there has been a conspicuous absence of experimental work. This may be attributed to two difficulties encountered in measuring the 1D drag. First, since it is a very small effect, the drag voltage usually has a very small magnitude and must be clearly distinguished from spurious signals. Second, and perhaps the major difficulty, has been the difficulty in creating parallel, electrically isolated, quantum wires with a spatial separation large enough to completely suppress interwire, while small enough to give a drag voltage of a reasonable magnitude. It was only recently that Debray *et al* [5]

reported the first experimental observation of Coulomb drag between ballistic quantum wires. The same authors later published a more comprehensive experimental work [6] on the subject. Work along the same lines has lately been reported by Yamamoto et al [7]. In the following, we give a brief outline of the reported experimental work and an analytical discussion of the results in the framework of the Fermi and the Luttinger liquid theory as discussed in Secs. II and III.

### *4.1. A. Experimental techniques for dual-wire sample realization*

The samples used for 1D Coulomb drag measurements consisted of two electrically isolated, parallel quantum wires, with a small spatial separation. Such samples were fabricated from AlGaAs/GaAs heterostructures with a high-mobility ($\cong 10^6 \mathrm{cm}^2/\mathrm{Vs}$) two-dimensional electron gas (2DEG) at the interface. The dual-wire samples were fabricated using high-resolution electron beam lithography, combined with deep chemical etching. The samples used so far were made in a planar geometry by depletion of a single 2DEG layer by three surface Schottky gates [5, 6, 7] deposited on the heterostructure wafer. Figure 5 gives a schematic top view of the planar device and the scanning electron micrograph of a typical device [6]. U, M, and L are surface Schottky gates.

**Figure 5.** (a) Schematic top view of a planar Coulomb drag device. U, M, and L are surface Schottky gates. (b) A scanning electron micrograph of a typical device with middle gate width of 50 nm.

Dual-wire samples for drag measurements can also be made in a vertical geometry [4] from two vertically stacked quantum well (QW) structures with a 2DEG in each well (such samples have not yet been used). The advantage of the planar geometry is that the interwire separation can be changed in-situ by changing the bias voltage of the central gate M. The disadvantage is that the narrow central gate creates a soft lateral potential barrier and to prevent tunneling between the wires the width of this barrier has to be of a sufficient magnitude, which sets a limit to the minimum interwire distance that can be used without electron tunneling interfering. Samples with a vertical geometry have been widely used for studying Coulomb drag between 2D electron layers [2]. The main advantage of the vertical geometry is that very small interwire separation (the barrier width) can be obtained without tunneling between wires. Since the magnitude of the drag is expected to decrease exponentially with interwire separation, one can expect to observe enhanced drag with the vertical samples because of the smaller separation that can be achieved with such samples. The major disadvantage is that the interwire separation cannot be changed in-situ, in contrast to the planar case. Also, it is not obvious that the widths of the two wires can be independently changed through the use of the mutually aligned top and bottom split gates.

*4.2. B. Experimental observation of Coulomb drag*

In their work, Debray et al [6] used a planar geometry of quantum wires, as shown in Fig. 5, of lithographic length $L$= 2 $\mu$m with a middle gate M of lithographic width 50 nm. The drag voltage $V_D$ was measured with a drive voltage $V_{DS}$ in the linear regime of ballistic electron transport as a function of the width of the drive wire by adjusting the bias voltage $V_U$, while the width of the drag wire was adjusted to have the Fermi level $E_F$ just above the bottom of its lowest 1D subband. An appropriate negative bias voltage $V_M$ was applied to the middle gate to ensure total absence of interwire tunneling. Measurements were done in the *absence* of any such tunneling. In Fig. 6a is shown the measured drag voltage $V_D$ as a function of the width of the drive wire. The drag voltage is found to show peaks, which occur in the rising parts between the plateaus of the drive wire conductance. This suggests that they occur when the 1D subbands of the wires are aligned and the Fermi wave vector $k_F$ is small. Measurements carried out in a magnetic field B = 0.86 Tesla perpendicular to the plane of the device shown in Fig.6(b) indicate identical behavior except that the magnitude of $V_D$ is enhanced almost by a factor of three.

**Figure 6.** The drag voltage $V_D$ and drive current $I$ as function of drive wire width at a drive voltage $V_{DS} = 300$ $\mu$V [6]. (a) In zero magnetic field with the upper wire as the drive wire. (b) In a magnetic field of 0.86 Tesla with the bottom wire as the drive wire.

In order to have unambiguous evidence that the observed drag voltage $V_D$ is indeed due to the Coulomb drag effect, the authors measured the dependence of $V_D$ and $R_D$ on the interwire separation and the temperature. Figure 7 shows the dependence of $V_{DM}$, the height of the first $V_D$ peak of Fig. 6b and the corresponding $R_D$ as function of the middle gate bias voltage $V_M$. The two quantum wires (Fig. 5) were spatially separated by an effective distance $d$ due to the depletion by $V_M$ of the 2DEG under the middle gate M. In the voltage range of interest, $d$ was experimentally found to vary almost linearly with $V_M$ according to

$$d = d_0 + \alpha\,(V_0 - V_M)\,, \tag{40}$$

where $V_0$ is the value of $V_M$ for which the 2DEG under M is just depleted and $\alpha$ gives the total spatial displacement of the two depletion edges of M with respect to its bias voltage. $d_0$ is a constant for the same device and is nominally equal to the lithographic width of the gate M. One can change $d$ by varying $V_M$. In Eq.(40), $V_0$ and $\alpha$ were determined experimentally. The dependence of $R_D$ on $V_M$ was found to be exponential and can be described well by the relation, $R_D \propto e^{\beta V_M}$, where $\beta \cong 14.2(9)V^{-1}$.

The temperature dependence of Coulomb drag is a crucial feature that can be used to probe which one of the two theoretical models, the FL or the LL theory, constitutes a more appropriate description of 1D Coulomb drag. Measurements, such as shown in Fig.

**Figure 7.** Dependence of the drag response on interwire separation $d$ via the middle gate voltage $V_M$ [6]. (a) The maximum $V_{DM}$ of the first drag peak of Fig. 6(b) as a function of $V_M$. (b) The natural logarithm of the corresponding drag resistance $R_D$ as a function of $V_M$. The dotted line is a linear fit to the data points.

6, carried out in the temperature range 60 mK - 1.2K are shown in Fig. 8. A decrease of $V_D$ with increasing temperature was observed. The dependence on temperature of the drag resistance $R_D$ corresponding to $V_{DM}$ is shown in Fig. 9 for both in the absence and presence of an applied magnetic field B. The temperature dependence can be described well by the power law, $R_D \propto T^x$, with $x$ = -0.77(2) and –0.73(6) for B = 0 and B = 0.86 Tesla, respectively. It is interesting to note that the data points at temperatures lower than 180 mK, for zero field, and 300 mK, for nonzero field, fall below the power-law curve, indicating a suppression of the drag effect.

**Figure 8.** The dependence of drag voltage on temperature [6]. (a) The drag voltage $V_D$ as a function of the width of the upper (drive) wire in zero magnetic field with $V_{DS}$ = 300 $\mu$V at 70, 180, 300, 450, and 900 mK, corresponding to curves in order of decreasing peak height. (b) The same as in (a) but in a magnetic field of 0.86 tesla with $V_{DS}$ = 50 $\mu$V at 60, 180, 300, 450, 900 mK, and 1.2K.

**Figure 9.** The temperature dependence of drag resistance $R_D$ corresponding to $V_{DM}$of the first drag peak of Fig. 8 in zero field (a) and in a field of 0.86 Tesla (b) [6]. Note that the data points at the low end of the temperature range fall below the power-law curve.

Lately, using a lateral sample geometry , very similar to that shown in Fig. 5a, Yamamoto et al [7] has reported the observation of Coulomb drag and the influence of an applied magnetic field on it. Their results corroborate those of Debray et al [5] [6]. In their work, Yamamoto et al also reported the observation of a negative drag. However, since the negative drag was observed only when the drive wire was completely pinched off, it is highly questionable if the effect observed is due to Coulomb drag.

### *4.3. C. Discussion*

The origin of the observed peaks in the drag voltage $V_D$ (Fig.6) can be understood when one considers Eqs. (16)-(21) of Sec. II. Since $V_D$ is directly proportional to the drag current $I_D$, $V_D$ will show maxima whenever any two 1D subband bottoms of the two wires line up and the Fermi wave vectors in the two wires are equal and small. As seen from Fig. 6, the occurrences of the drag peaks correspond to these conditions. The first peak in $V_D$ occurs when the Fermi level is just above the bottoms of the lowest 1D

subbands of both wires. Similarly, the second peak occurs when the lowest subband of the drag wire lines up with the second subband of the drive wire. Both the increase and the narrowing of the first drag peak in a magnetic field of 0.86 Tesla (Fig 6(b)) can be attributed to an increase of the density of states in1D the subbands due to the magnetic-field-induced enhancement of the electron effective mass. The reduction in the magnitude of the drag peak as we move away from the first peak toward higher values of $V_U$ can be attributed to an increase in the effective interwire separation of the wires. This dependence is explained in detail later. Since we are mainly concerned with 1D transport in the fundamental mode, we restrict our discussion here to the region of the first drag peak.

To understand the dependence of drag on the interwire distance shown in Fig. 7, we note that the matrix element of the backscattering probability depends on the interwire distance $d$ via the modified Bessel function $K_0(2k_Fd)$ (Sec. II, Eq.(11)), which is an exponential function of its argument for $2k_Fd >> 1$. The same dependence also results from the LL theory [29]. Under this condition, an exponential decrease of $R_D$ with $d$ is expected according to $R_D \propto \exp(-4k_Fd)$. This is consistent with the results of Fig.7. Using the experimentally determined values $\beta = 14.2$ $V^{-1}$ and $V_0$ = -0.4V, $\alpha = 580$ nm $V^{-1}$, we find $k_F = 6.1$ x $10^6$ $m^{-1}$. Surprisingly, this corresponds to a low density of about 8 electrons per 2$\mu$m wire segment and a mean electron distance $\bar{r} \approx 250nm$ in the wire. When $V_M$ is in the range from -0.7 to –0.8 V, we have (Eq. (40) $d \cong 0.2$ $\mu$m. This gives $2k_Fd \cong 3$, so the approximation of $2k_Fd \gg 1$ is reasonable. This exponential decrease of $R_D$ with $d$ also explains why the height of the drag voltage peaks in Fig.6 decreases so rapidly as $V_U$ increases. An increase in $V_U$ increases the width of the drive wire and hence $d$. The decrease of $R_D$ for $V_M > -0.7V$ occurs due to tunneling of a considerable fraction of the current from the drive wire to the drag one, reducing the measured $R_D$.

The experimental observed features of the drag effect discussed above, namely, the origin of the drag voltage peaks, the effect the magnetic field, and the interwire separation dependence, can all be understood in the framework of both the FL and the LL theory. It is the temperature dependence of the drag that is the crucial feature - it can be used to determine which one of the two theoretical models constitutes a more appropriate description of 1D Coulomb drag observed under the given experimental conditions. The observed temperature dependence of $R_D$, shown in Fig.9, is in sharp contrast with the linear temperature dependence predicted by the FL theory (Eq. (19)). The unusual temperature dependence can not be attributed to a temperature induced modification of the wire conductance, since the latter is found to be almost unchanged over the temperature range of the measurements. A reduction of the interwire Coulomb coupling due to enhanced screening by the reservoirs and gates is very unlikely at such small temperatures. On the other hand, it's conceivable that a correlated LL behavior is established in the wires. Indeed, it is hardly surprising that the temperature dependence of $R_D$ does not fit into a FL scenario, because for the experimental condition of the first drag peak the ratio $r_s$ of $\bar{r}$ and the Bohr radius $a_B$, $r_s = \bar{r}/a_B \approx 26$ is large.

The smallness of the drag resistance ($R_D < 100\Omega$) in zero magnetic field indicates a weak interwire back scattering coupling. In this case, according to the LL model $R_D$ should obey a power law as long as the thermal length $L_T$ is well in between the wire length $L = 2$ $\mu$m and the mean electron distance $\bar{r} \approx 250nm$ in the wire. For spin-unpolarized electrons, valid for the data shown in Fig.9, the LL description predicts a power-law temperature dependence of $R_D$ with exponent $x = 2K_{c-} - 1$ (Eq.(38)). The data shown in Fig.9 indeed shows a power-law dependence of $R_D$ on temperature with $K_{c1} = 0.12$. Let us see if the condition $\bar{r} < L_T < L$ is fulfilled in the experiment. Given a Fermi wavevector of $k_F \approx 6\mu m^{-1}$ we find that $L_T = hv_F/K_{c-}k_BT$ is equal to the wire length $L = 2$ $\mu$m at a temperature $T_L \cong 250$ mK, and that $L_T$ approaches $\bar{r} \approx 250nm$ at a temperature of about 2K. Here $v_F/K_{c-}$ is the group velocity of the relative electron-density fluctuations and $h/k_BT$ is the quantum lifetime associated with the thermal energy $k_BT$. This means that there is a narrow temperature range window in which a power-law temperature dependence of $R_D$ might be expected, and it is observed experimentally. At temperatures below $T_L$, when $L < L_T$,the electron coming from the lead to the wire does not have time to accommodate itself to the LL liquid. This should result in a drag weaker than the power-law dependence. The experimental data of Fig.9 are consistent with this analysis. At lower temperatures we do indeed observe a tendency to a weakening of the drag with respect to the power-law dependence.

The negative power-law temperature dependence is not the only experimental feature that can not be understood in terms of the FL theory of Coulomb drag. The experimental value of $R_D$ (Fig. 9a) at T = 60 mK is more than an order of magnitude larger than that given by FL theory (Eq. (19)). That the measured drag is larger could be explained by the interaction-normalized interwire backscattering probability, which should be larger than the bare one (Eq. (34)).

Comparison of Figs. 9(a) and 9(b) show that the influence of the magnetic field on the temperature dependence is not significant. This may signify that Zeeman spin splitting at B $\leq$ 1 Tesla is not important yet, otherwise the exponent $x$ should change (Eq. (35)). Indeed, a clear signature of spin splitting in the measured conductance staircase was not observed at this field. The magnetic field, however, increases $v_F$ for the same position of the Fermi level. This makes $L_T$ larger at the same temperature compared to that in zero field. This can explain why in a magnetic field a deviation from the power-law dependence occurs at a higher temperature (Fig.9(b)).

We have interpreted above the experimental data in terms of Coulomb drag only. Considering the large interwire separation for which the drag measurements were made, one can not rule out the possibility of an acoustic phonon-mediated drag (PMD) contribution to the measured drag resistance. Recent theoretical work [45] [46] on 1D PMD based on Fermi liquid description predicts that PMD is negligible compared to Coulomb drag for $2k_Fd < 5$. Also, for a dual-wire sample shown in Fig.5, $R_D$ should increase exponentially with temperature in the range 100 - 600 mK and does not decrease exponentially with interwire separation $d$. The data shown in Figs.7 and 9 qualitatively contradict these predictions. This allows us to conclude that the PMD contribution, if

present at all, is insignificant.

## 5. V. Future prospects

It is quite obvious from the content of Sec. IV that substantial experimental work remains to be done to gain a comprehensive understanding of the physics of Coulomb drag between interacting 1D electron systems and to explore the conditions under which such systems behave as a Fermi liquid or a Luttinger liquid. Since the measurement of the Coulomb drag also provides a new experimental tool to probe the LL state that can't be done from the measurement of the conductance alone, extensive experimental work on the subject is needed to put the LL model of interacting 1D systems on a firm footing. Though the theory of Coulomb drag has considerably outstripped experimental work, many open questions need to be addressed in the theoretical area as well.

On the experimental side, work should be focused on measurements that can distinguish between a LL and a FL state and can provide information about the existence and the nature of the LL state. This is an extremely important area for condensed matter physics. The few papers published so far, claiming to have observed a Luttinger liquid, have not been convincing. In this respect, it would be highly interesting to study the drag between spin polarized systems, since the LL theory predicts different exponents for spin polarized and unpolarized cases and manifestation of the spin effect should be quite different in the Fermi liquid and the Luttinger liquid state. Another interesting experimental possibility is to study drag when the wire length $L$ falls below the thermal length $L_T$ to investigate if the drag resistance $R_D$ decays $\propto \quad T^2$ as predicted by LL liquid theory. When the number of electrons in the wires is very small (Sec. IV), one should expect relatively large fluctuations of the drag current or voltage, such as shot noise [47][48], and possible reversal of the sign of drag leading to negative drag [49]. Observation of this noise can also provide valuable information on correlated electron state. One could also envision a search for 1D spin Coulomb drag [50]. Finally, it is also important to study acoustic phonon-mediated drag (PMD) [45] [46] since under certain conditions it can be comparable to and even larger than the Coulomb drag. If such a PMD is present in the experimental measurements, one has to find ways to separate it from the Coulomb drag.

The theory of Coulomb drag based on the LL model is far from mature and many open questions need to be addressed such as the effect of disorder, the influence of tunneling between the wires, etc.. Alhough the power-law temperature dependence of the drag resistance is a signature of the Luttinger liquid state, a careful analysis of various limiting cases based on the Fermi liquid approach should be carried out to make sure that under no circumstances it can give a similar temperature dependence. It is equally important to investigate the physical situations and interactions (within the wires and with the reservoirs) that favor transition of the Fermi liquid into the Luttinger liquid and vice versa.

[1] Pogrebinskii M B 1977 *Sov. Phys. Semicond.* **11** 372
[2] For a recent review see Rojo A 1999 *J. Phys : Condens. Matter* **11** R31
[3] Nozieres P 1997 *Theory of Interacting Fermi Systems* (Addison-Wesley)
[4] Moon J S, Blount M A, Simmons J, Wendt J R, Lyo S K and Reno J L 1999 *Phys. Rev.* B **60** 11530
[5] Debray P, Vasilopoulos P, Raichev O, Perrin R, Rahman M and Mitchel W C 2000 *Physica* E **6** 694
[6] Debray P, Zverev V, Raichev O, Klesse R, Vasilopoulos P and Newrock R S 2001 *J. Phys.: Condens. Matter* **13** 3389
[7] Yamamoto M, Stopa M, Tokura Y, Hira yama Y and Tarucha S 2001 *Proceedings of the $25^{th}$ Intl. Conf. On the Physics of Semiconductors* (World Scientific)
[8] Gurevich V L, Pevzner V B, Fenton E W 1998 *J. Phys.: Condens. Matter* **10** 2551
[9] Sirenko Y M and Vasilopoulos P 1992 *Phys. Rev.* B **46** 1611
[10] Ben Yu-Kuang Hu and Karsten Flensberg, in *Hot Carriers in Semiconductors*, edited by K. Hess et al., Plenum Press, New York, 1996.
[11] B. Tanatar, Phys. Rev. B **58**, 1154 (1998).
[12] A. Komnik, R. Egger, Phys. Rev. Lett. **80**, 2881 (1998).
[13] K. Flensberg, Phys. Rev. Lett. **81**, 184 (1998).
[14] Raichev O and Vasilopoulos P 2000 *Phys. Rev.* B **61** 7511
[15] Nazarov Y V and Averin D V 1998 *Phys. Rev. Lett.* **81** 653
[16] Ponomarenko V V and Averin D V 2000 *Phys. Rev. Lett.* **85** 4928
[17] Klesse R and Stern A 2000 *Phys. Rev.* B **62** 16912
[18] Gurevich V L and Muradov M I 2000, Pis'ma v ZhETF **71**, 164 [JETP Letters **71**, 111]
[19] Haldane F D M 1981 *J. Phys.* C **14** 2585; Haldane F D M 1981 *Phys. Rev. Lett.* **47** 1840
[20] Voit J 1994 *Rep. Prog. Phys.* **57** 977
[21] Bockrath M, Cobden D H, Lu J, Rinzler A G, Smalley R E, Balents L, McEuen P L 1999 *Nature* **397** 598
[22] Auslander O M, Yacoby A, Picciotto R de, Baldwin k W, Pfeiffer L N and West k W 2000 *Phys. Rev. Lett.* **84** 1764
[23] Takiainen, Ahlskog M, Penttila J, Roschier L, Hakonen P, Paalanen M and Sonin E 2001 *Phys. Rev.* B **64** 195412
[24] Auslander O M, Yacoby A, Picciotto R de, Baldwin k W, Pfeiffer L N and West k W 2002, Science **295** 825
[25] Tsukagoshi K, Alphenar B W and Nakazato K 1998 *Appl. Phys. Lett.* **73** 2515
[26] Amlani I, Orlov A O, Snider G L, Lent C S and Bernstein H G 1998 *Appl. Phys. Lett.* **72** 2179
[27] Gurevich L E 1945 *Journ. of Phys. USSR* **9**, 477
[28] Landauer R 1989 *IBM J. Res. Develop.* **32** 306
[29] Imry Y 1986 *Directions in Condensed Matter Physics* (World scientific)
[30] Buttiker M 1986 *Phys. Rev.Lett.* **57** 1761
[31] Velicky B, Špička V and Masek J 1989 *Sol. Stat. Comm.* **72** 981
[32] Gurevich V L, Pevzner V B and Hess K 1994 *J. Phys. : Condens. Matter* **6** 8363
[33] Gurevich V L, Pevzner V B and Hess K 1995 *Phys. Rev.* B **51** 5219
[34] Gurevich V L, Pevzner V B and Iafrate G J 1995 *Phys. Rev. Lett.* **75** 1352
[35] Gradshtein I S and Ryzhik 1980 *Tables of Integrals Series and Products* (Academic Press)
[36] Gurevich V L, Muradov M I, unpublished
[37] Tomonaga S 1950 *Progr. Theor. Phys.* **5** 544; Luttinger J M 1963 *J. Math. Phys.* **4** 1154
[38] Emery V J 1979 *Highly Conducting One-Dimensional Solids* (Plenum)
[39] Solyom J 1978 *Adv. Phys.* **28** 201
[40] Schulz H J, Cuniberti G and Pieri P 1997 *Fermi Liquids and Luttinger Liquids*, Lecture Notes of the Chia laguna Summer School, Italy
[41] Creffield C E, Häusler W and MacDonald A H 2001 Europhys. Lett **53** 221

[42] Häusler W, Kecke L, and MacDonald A H 2002 Phys. Rev. B **65** 085104
[43] Klesse R and Stern A, *unpublished*
[44] Luther A and Emery V J 1974 *Phys. Rev. Lett.* **33** 589; Chui S T and Lee P A 1975 *Phys. Rev. Lett.* **35** 315
[45] Raichev O E 2001 *Phys. Rev.* B **64** 035324
[46] Muradov M I 2001 *cond-mat/*0107622
[47] Gurevich V L and Muradov M I 2000 *Phys. Rev.* B **62** 1576
[48] Trauzettel B, Egger R and Grabert H 2002 *Phys. Rev. Lett.* **88** 116401
[49] Mortensen N A, Flensberg K and Jauho A-P 2002 *Phys. Rev.* B **65** 085317
[50] D'Amico I and Vignale G 2002, Phys. Rev. B **65** 085109

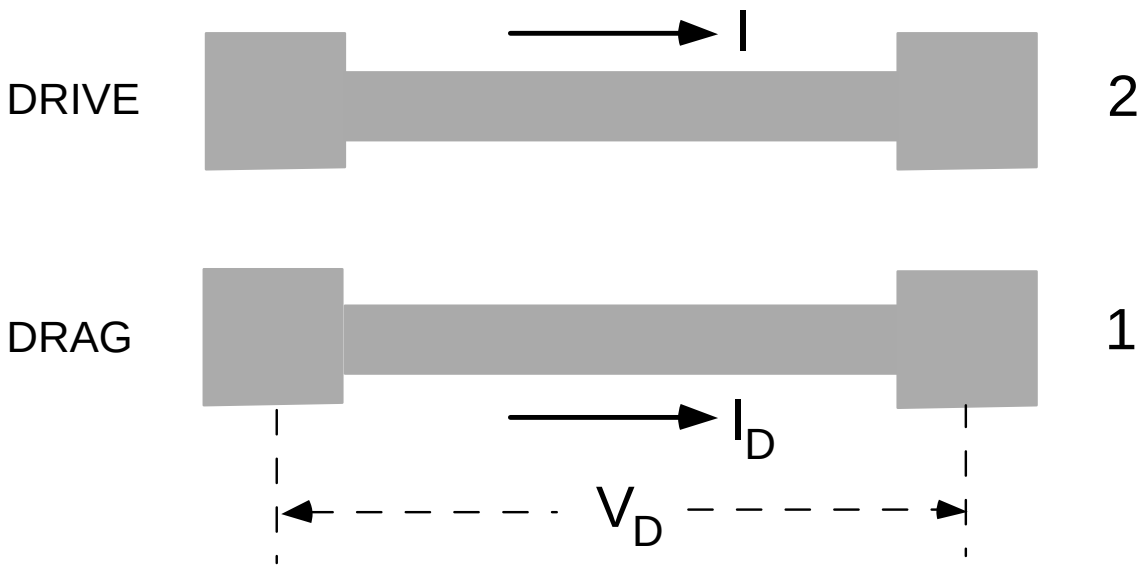


Fig. 1
P. Debray et al.

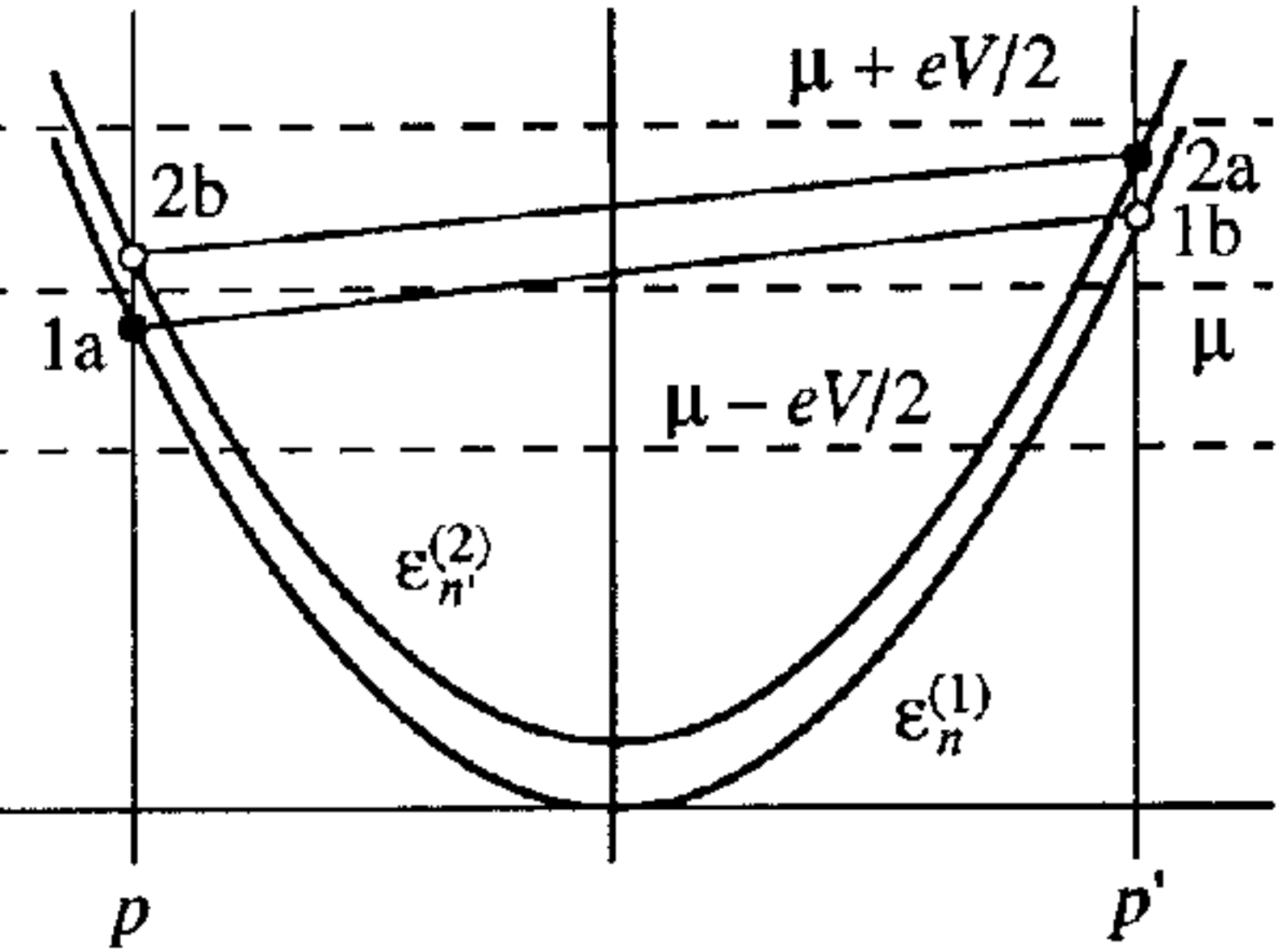
μ + eV/2
2b
2a
1b
1a
μ
μ − eV/2
$\varepsilon_{n'}^{(2)}$
$\varepsilon_{n}^{(1)}$
p
p'

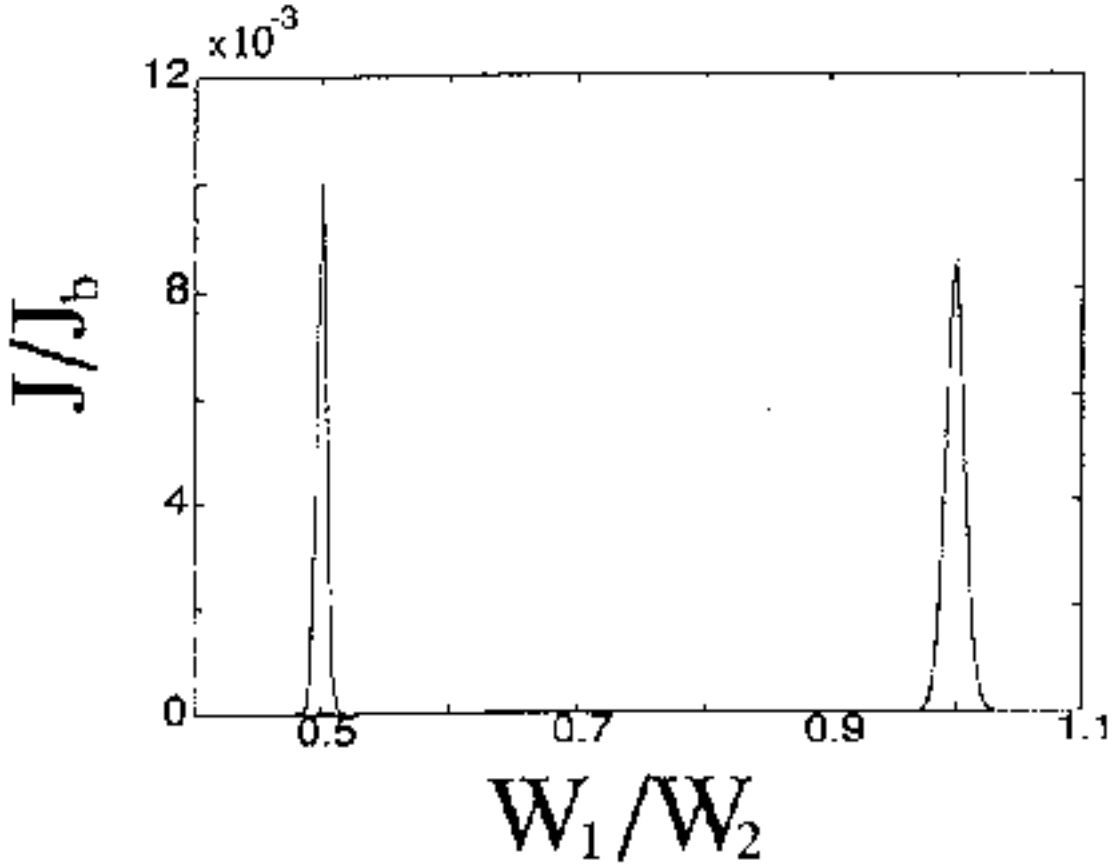
x10^-3
12
8
4
0
J/J_b
0.5
0.7
0.9
1.1
W_1 /W_2

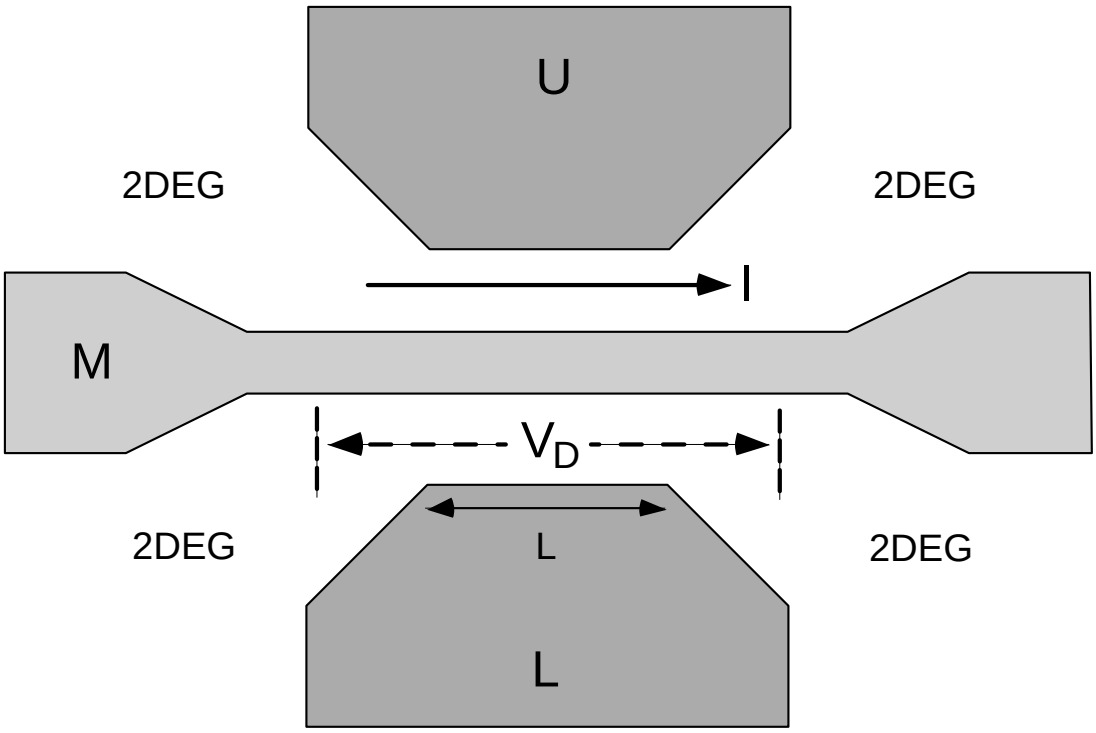


Fig. 5 (a)
P. Debray et al.

This figure "fig5b.jpg" is available in "jpg"  format from:

http://arXiv.org/ps/cond-mat/0207408v1

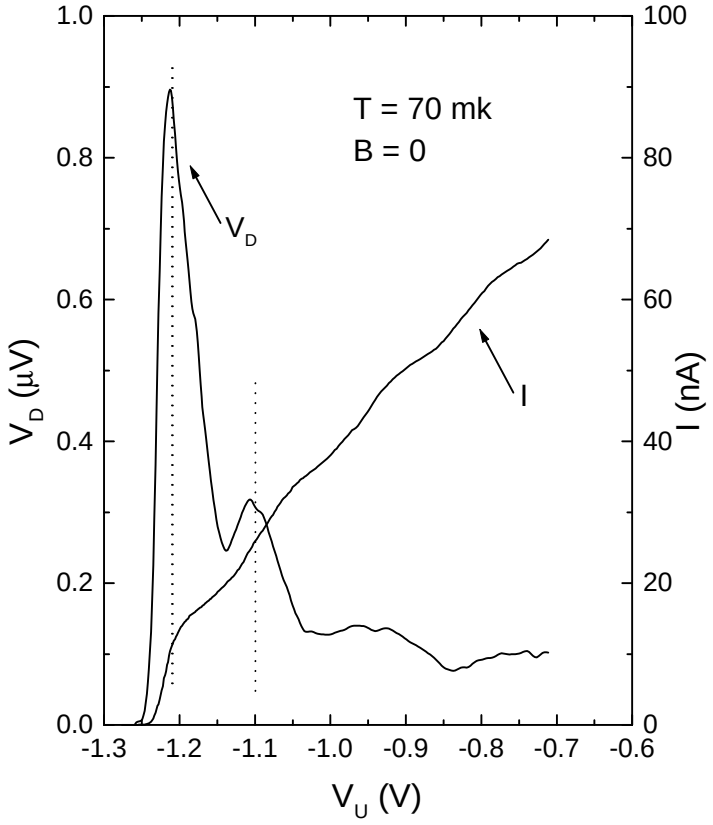


Fig. 6(a)
P. Debray et al.

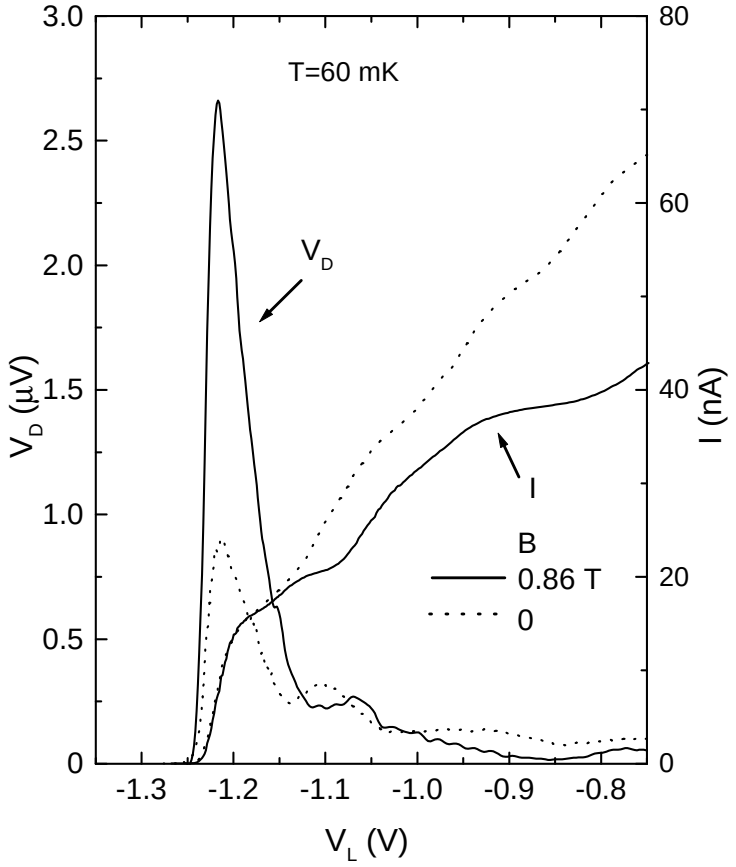


Fig. 6(b)
P. Debray et al.

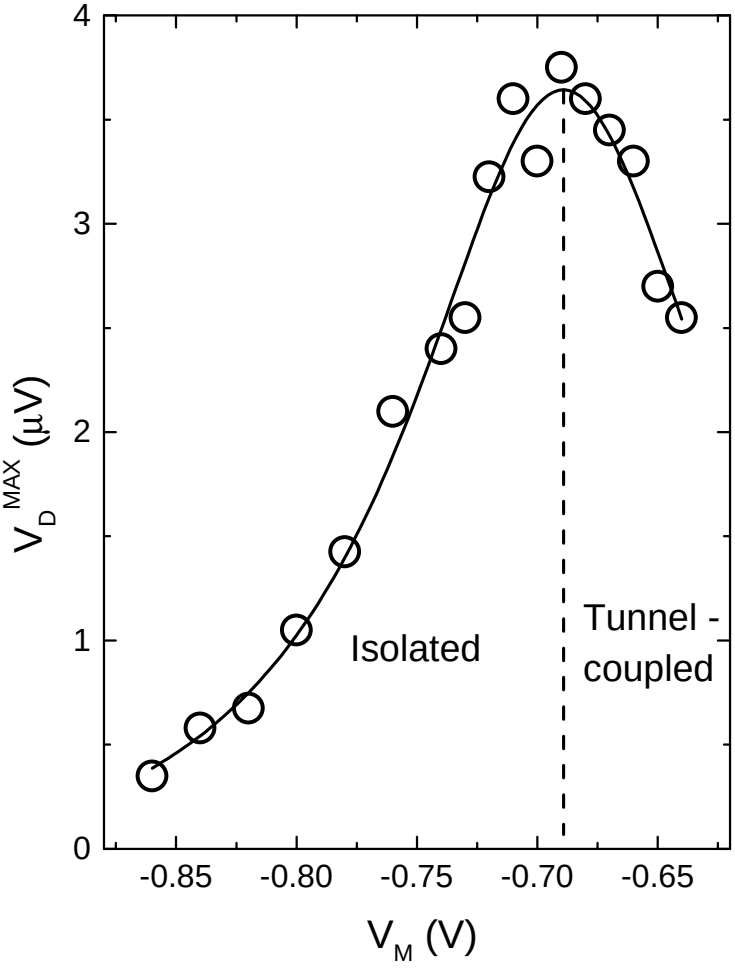


Fig. 7(a)
P. Debray et al.

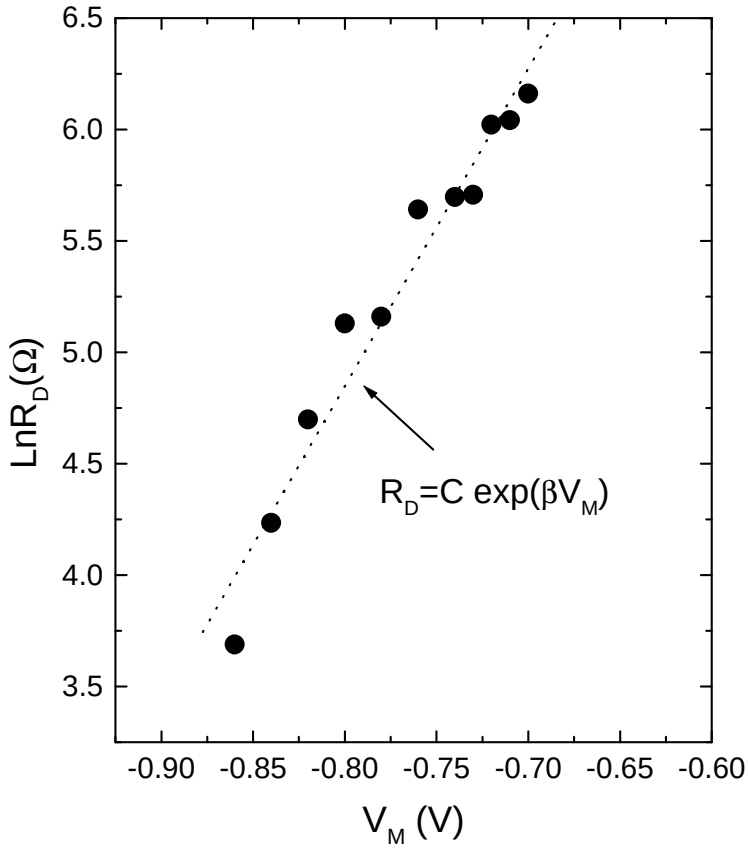


Fig. 7(b)
P. Debray et al.

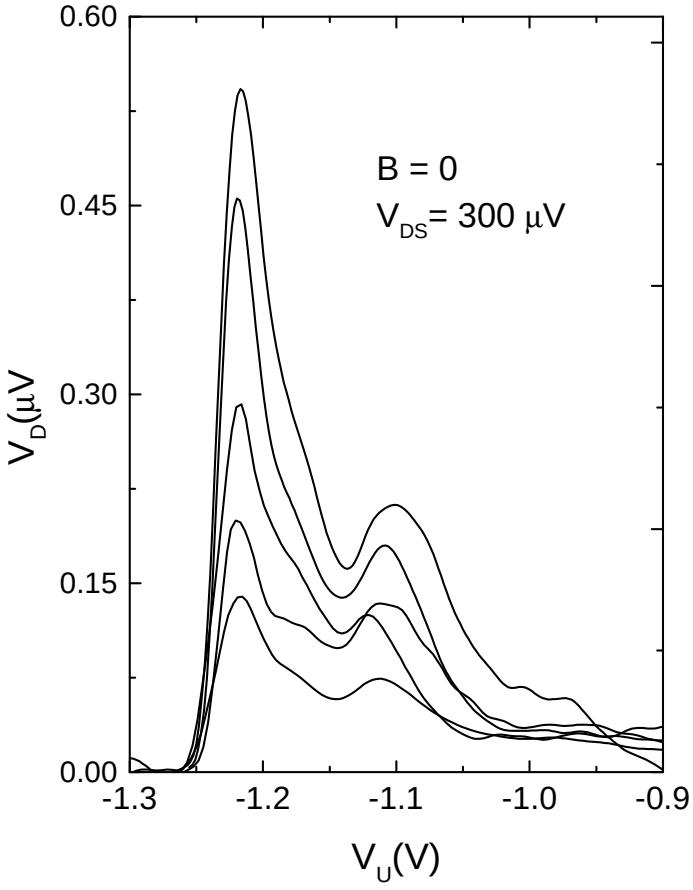


Fig. 8(a)
P. Debray et al.

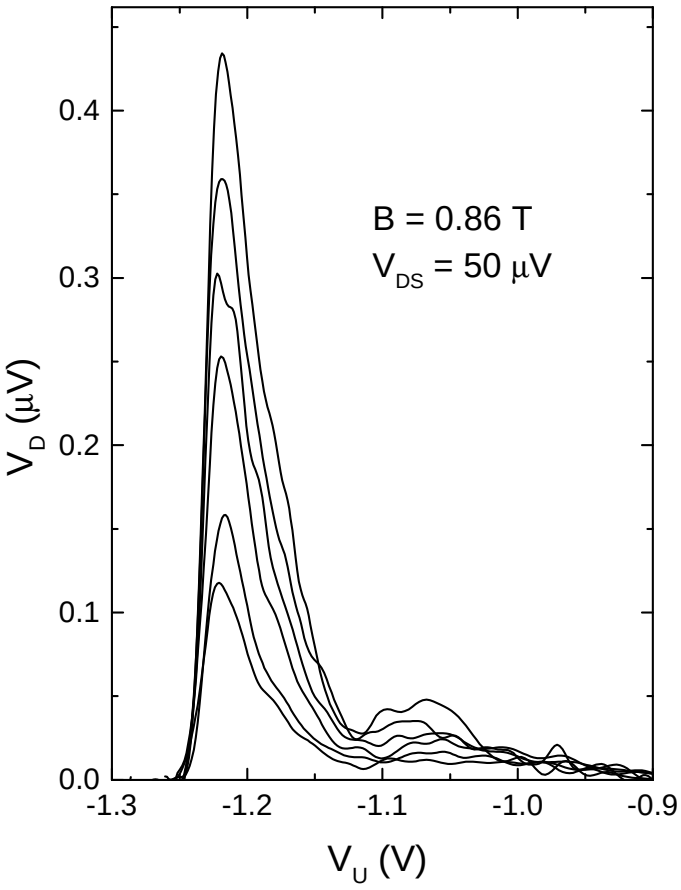


Fig. 8(b)
P. Debray et al.

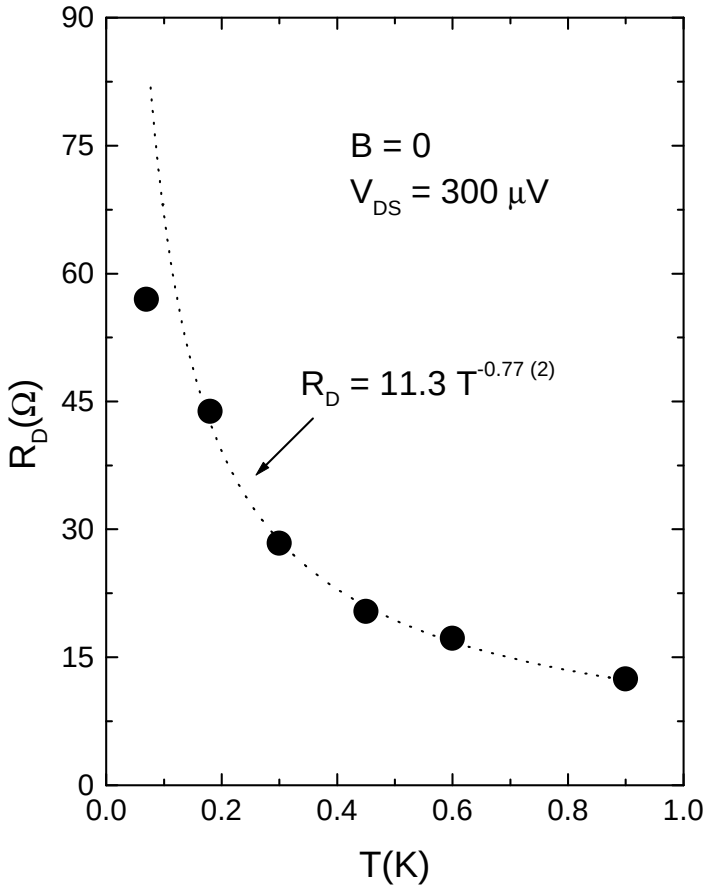


Fig. 9(a)
P. Debray et al.

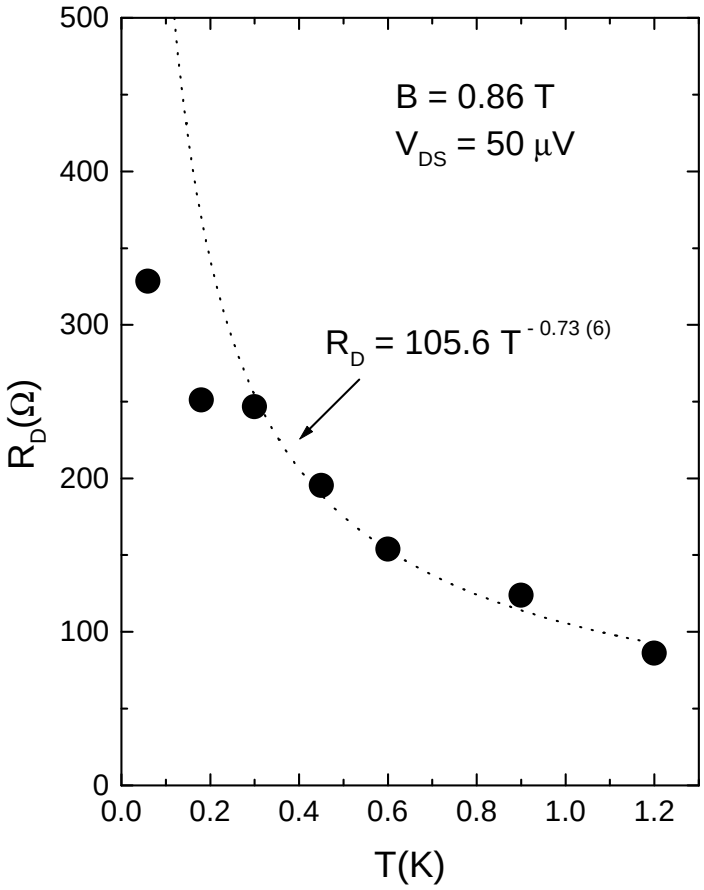


Fig. 9(b)
P. Debray et al.